

1 **Water adsorption and hygroscopic growth of six anemophilous pollen species: the**  
2 **effect of temperature**

3  
4 Mingjin Tang,<sup>1,5,6,\*</sup> Wenjun Gu,<sup>1,5</sup> Qingxin Ma,<sup>2,5,6,\*</sup> Yong Jie Li,<sup>3</sup> Cheng Zhong,<sup>2,5</sup> Sheng Li,<sup>1,5</sup>  
5 Xin Yin,<sup>1,5</sup> Ru-Jin Huang,<sup>4</sup> Hong He,<sup>2,5,6</sup> Xinming Wang<sup>1,5,6</sup>

6  
7 <sup>1</sup> State Key Laboratory of Organic Geochemistry and Guangdong Key Laboratory of  
8 Environmental Protection and Resources Utilization, Guangzhou Institute of Geochemistry,  
9 Chinese Academy of Sciences, Guangzhou 510640, China

10 <sup>2</sup> State Key Joint Laboratory of Environment Simulation and Pollution Control, Research Center  
11 for Eco-Environmental Sciences, Chinese Academy of Sciences, Beijing 100085, China

12 <sup>3</sup> Department of Civil and Environmental Engineering, Faculty of Science and Technology,  
13 University of Macau, Avenida da Universidade, Taipa, Macau, China

14 <sup>4</sup> Key Laboratory of Aerosol Chemistry and Physics, State Key Laboratory of Loess and  
15 Quaternary Geology, Institute of Earth and Environment, Chinese Academy of Sciences, Xi'an  
16 710061, China

17 <sup>5</sup> University of Chinese Academy of Sciences, Beijing 100049, China

18 <sup>6</sup> Center for Excellence in Regional Atmospheric Environment, Institute of Urban Environment,  
19 Chinese Academy of Sciences, Xiamen 361021, China

20

21 \* Correspondence: Mingjin Tang (mingjintang@gig.ac.cn), Qingxin Ma (qxma@rcees.ac.cn)

22

## 23 **Abstract**

24 Hygroscopicity largely affects environmental and climatic impacts of pollen grains, one  
25 important type of primary biological aerosol particles in the troposphere. However, our knowledge  
26 in pollen hygroscopicity is rather limited, and especially the effect of temperature has rarely been  
27 explored before. In this work three different techniques, including a vapor sorption analyzer,  
28 diffusion reflectance infrared Fourier transform spectroscopy (DRIFTS) and transmission Fourier  
29 transform infrared spectroscopy (transmission FTIR) were employed to characterize six  
30 anemophilous pollen species and to investigate their hygroscopic properties as a function of  
31 relative humidity (RH, up to 95%) and temperature (5 or 15, 25 and 37 °C). Substantial mass  
32 increase due to water uptake was observed for all the six pollen species, and at 25 °C the relative  
33 mass increase at 90% RH, when compared to that at <1% RH, ranged from ~30 to ~50%, varying  
34 with pollen species. **It was found that the** modified  $\kappa$ -Köhler **equation** can well approximate mass  
35 hygroscopic growth of all the six pollen species, and the single hygroscopicity parameter ( $\kappa$ ) was  
36 determined to be in the range of  $0.034\pm 0.001$  to  $0.061\pm 0.007$  at 25 °C. In-situ DRIFTS  
37 measurements suggested that water adsorption by pollen species was mainly contributed by OH  
38 groups of organic compounds they contained, and good correlations were indeed found between  
39 hygroscopicity of pollen species and the amount of OH groups, as determined using transmission  
40 FTIR. Increase in temperature would in general lead to decrease in hygroscopicity, except for  
41 pecan pollen. For example,  $\kappa$  values decreased from  $0.073\pm 0.006$  at 5 °C to  $0.061\pm 0.007$  at 25 °C  
42 and to  $0.057\pm 0.004$  at 37 °C for populus tremuloides pollen, and decreased from  $0.060\pm 0.001$  at  
43 15 °C to  $0.054\pm 0.001$  at 25 °C to  $0.050\pm 0.002$  at 37 °C for paper mulberry pollen.

44

## 45 **1 Introduction**

46 Primary biological aerosol particles (PBAPs), an important type of aerosol particles in the  
47 troposphere, are directly emitted from the biosphere and include pollen, fungal spores, bacteria,  
48 viruses, algae, and so on (Després et al., 2012; Fröhlich-Nowoisky et al., 2016). Emission and  
49 abundance of PBAPs are quite uncertain, and annual emission fluxes are estimated to be in the  
50 range of <10 to ~1000 Tg for total PBAPs and 47-84 Tg for pollen (Després et al., 2012). Pollen,  
51 and PBAPs in general, are of great concerns due to their various impacts on the Earth system (Sun  
52 and Ariya, 2006; Ariya et al., 2009; Georgakopoulos et al., 2009; Morris et al., 2011; Morris et al.,  
53 2014; Fröhlich-Nowoisky et al., 2016). For example, they can be allergenic, infectious or even  
54 toxic, affecting the health of human and other species in the ecological systems over different  
55 scales (Douwes et al., 2003; Reinmuth-Selzle et al., 2017; Shiraiwa et al., 2017). The geographical  
56 dispersion of anemophilous plants largely relies on pollen dispersal, which in turn depends on the  
57 emission, transport and deposition of pollen grains; therefore, pollen plays a key role in the  
58 evolution of many ecosystems (Womack et al., 2010; Fröhlich-Nowoisky et al., 2016). In addition,  
59 PBAPs can serve as giant cloud condensation nuclei (CCN) and ice nucleating particles (INPs),  
60 significantly impacting the formation and properties of clouds and thus radiative balance and  
61 precipitation (Möhler et al., 2007; Ariya et al., 2009; Pratt et al., 2009; Pope, 2010; Pummer et al.,  
62 2012; Gute and Abbatt, 2018). It has also been proposed that PBAPs may have significant impacts  
63 on chemical composition of aerosol particles via heterogeneous and multiphase chemistry  
64 (Deguillaume et al., 2008; Estillore et al., 2016; Reinmuth-Selzle et al., 2017; Shiraiwa et al., 2017).

65 Hygroscopicity is one of the most important physicochemical properties of pollen (as well  
66 as aerosol particles in general). Hygroscopicity largely impacts the transport and deposition of  
67 pollen grains (Sofiev et al., 2006), therefore affecting their lifetimes, abundance and

68 spatiotemporal distribution. In addition, hygroscopicity is closely linked to the ability of aerosol  
69 particles to serve as CCN and INPs (Petters and Kreidenweis, 2007; Kreidenweis and Asa-Awuku,  
70 2014; Laaksonen et al., 2016; Tang et al., 2016). Several previous studies have measured the  
71 hygroscopicity and CCN activities of pollen (Diehl et al., 2001; Pope, 2010; Griffiths et al., 2012;  
72 Lin et al., 2015; Steiner et al., 2015; Prisle et al., 2018) and other PBAPs such as bacteria (Pasanen  
73 et al., 1991; Reponen et al., 1996; Franc and DeMott, 1998; Ko et al., 2000; Lee et al., 2002; Bauer  
74 et al., 2003). For example, water uptake of eleven pollen species was studied using an analytical  
75 balance (Diehl et al., 2001), and the mass of pollen was found to be increased by 3-16% at 73%  
76 RH and by ~100-300% at 95% RH, compared to that at 0% RH. An electrodynamic balance was  
77 employed to investigate hygroscopic growth of eight types of pollen (Pope, 2010; Griffiths et al.,  
78 2012), and it was found that their hygroscopic growth can be approximated by the modified  $\kappa$ -  
79 Köhler **equation**, with single hygroscopicity parameters being around 0.1 (depending on the  
80 assumed pollen density, **as discussed in Section 3.2**).

81 Previous measurements were mostly carried out at or close to room temperature, and the  
82 effects of temperature on hygroscopic properties of pollen and other types of PBAPs are yet to be  
83 elucidated. To our knowledge, only one previous study (Bunderson and Levetin, 2015) explored  
84 the effect of temperature (4, 15 and 20 °C) on water uptake by *Juniperus ashei*, *Juniperus*  
85 *monosperma* and *Juniperus pinchotii* pollen. It is important to account for the temperature effects,  
86 because ambient temperatures range from below -70 to >30 °C **in the troposphere**. In particular,  
87 the altitude of 0.5-2.0 km to which pollen can be easily transported (Noh et al., 2013) may have  
88 temperatures close to or lower than the chilling temperatures for vegetative species (up to 16.5 °C)  
89 (Melke, 2015). Moreover, the temperature in the respiratory tract can reach up to of 37 °C (the  
90 physiological temperature). In the work presented here, a vapor sorption analyzer (VSA) was

91 employed to investigate hygroscopic growth of pollen grains at different temperature (5 or 15, 25,  
92 and 37 °C), a range covering the chilling temperature to the physiological temperature. Water  
93 uptake by pollen was also examined using diffusion reflectance infrared Fourier transform  
94 spectroscopy at room temperature to complement the VSA results. Furthermore, transmission  
95 Fourier transformation infrared spectroscopy was used to characterize functional groups of dry  
96 pollen grains, in an attempt to seek potential links between chemical composition of pollen grains  
97 and their hygroscopic properties.

## 98 **2 Experimental sections**

99 Six pollen species, all from anemophilous plants, were investigated in this work, including  
100 populus tremuloides and populus deltoides (provided by Sigma Aldrich) as well as ragweed, corn,  
101 pecan and paper mulberry (provided by Polysciences, Inc.). **The six pollen species were chosen in  
102 our work primarily because they were commercially available. Furthermore, these plants are also  
103 widely distributed in the globe. For example, corn is the most produced grain in the world  
104 (International-Grains-Council, 2019), and up to 50% of pollen-related allergic rhinitis cases in  
105 North America are caused by ragweed pollen (Taramarcaz et al., 2005).**

### 106 **2.1 Fourier transformation infrared spectroscopy**

107 The adsorption of water by pollen species were studied using in-situ diffusion reflectance  
108 infrared Fourier transform spectroscopy (DRIFTS) at room temperature (~25 °C). This technique  
109 was described in details in our previous work (Ma et al., 2010), and similar setups have also been  
110 used by other groups to investigate adsorption of water by mineral dust (Joshi et al., 2017; Ibrahim  
111 et al., 2018). Infrared spectra were recorded using a Nicolet 6700 Fourier transformation infrared  
112 spectrometer (FTIR, Thermo Nicolet Instrument Corporation), equipped with an in-situ diffuse  
113 reflection chamber and a high-sensitivity mercury cadmium telluride (MCT) detector cooled by

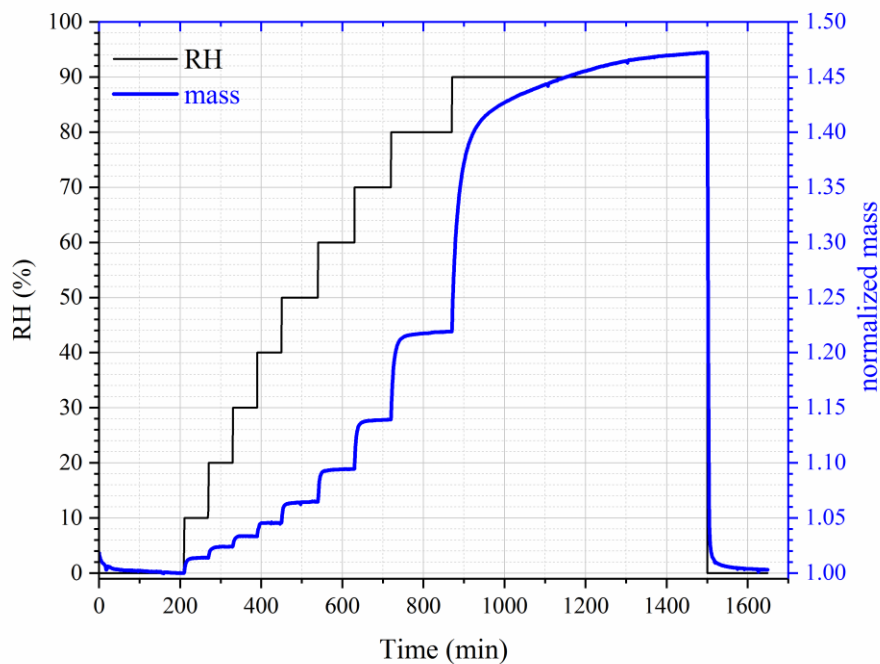
114 liquid nitrogen. A pollen sample (about 10 mg for each sample) under investigation was placed  
115 into a ceramic crucible which was located in the in-situ chamber. A dry air flow and a humidified  
116 air flow were first mixed and then delivered into the chamber, and the total flow rate was set to  
117 200 mL/min (standard condition). Relative humidity (RH) in the chamber could be adjusted by  
118 varying the flow rate ratio of the dry flow to the humidified flow, and was monitored online using  
119 a moisture meter (CENTER 314) with an absolute uncertainty of  $\pm 2\%$ . Prior to each experiment,  
120 the sample was flushed with dry air for 3 h at 25 °C, and the reference spectrum was recorded after  
121 the pretreatment. Infrared spectra were collected and analyzed using OMNIC 6.0 software (Nicolet  
122 Corp.). All the spectra reported here were recorded with a wavenumber resolution of  $4\text{ cm}^{-1}$ , and  
123 100 scans were averaged to produce a spectrum. Water adsorption was equilibrated for at least 30  
124 min at each RH to ensure that the equilibrium between water vapor and adsorbed water was  
125 reached.

126 Pollen samples used in this work were also characterized using transmission FTIR  
127 equipped with a deuterated triglycine sulfate detector (DTGS) detector. Pollen grains and KBr  
128 were mixed with a mass ratio of approximately 1:100 and ground in an agate mortar, and the  
129 mixture was then pressed into a clear disc. Transmission FTIR was employed to examine these  
130 discs, and a pure KBr disc was used as the reference. All the spectra, each of which was the average  
131 of 100 scans, were also recorded with a wavenumber resolution of  $4\text{ cm}^{-1}$ .

## 132 **2.2 Vapor sorption analyzer**

133 Hygroscopic growth of pollen grains was further investigated using a vapor sorption  
134 analyzer (Q5000 SA, TA Instruments, New Castle, DE, USA) described in our previous work (Gu  
135 et al., 2017; Guo et al., 2018; Jia et al., 2018). In brief, this instrument measured the sample mass  
136 as a function of RH under isothermal conditions. The instrument can be operated in the temperature

137 range of 5-85 °C with a temperature accuracy of  $\pm 0.1$  °C and in the RH range of 0-98 % with an  
138 absolute accuracy of  $\pm 1\%$ . RH in the humidity chamber was regulated by using two mass flow  
139 controllers to control the dry and humidified nitrogen flows very precisely. The accuracy in RH  
140 control was routinely checked by measuring the DRH values for a series of standard compounds,  
141 e.g., NaCl,  $(\text{NH}_4)_2\text{SO}_4$ , KCl, and etc., and the difference between the measured and theoretical  
142 DRH was always  $< 1\%$ . The mass measurement had a range of 0-100 mg and a sensitivity of  $\pm 0.01$   
143  $\mu\text{g}$ . The initial mass of each sample used in this work was in the range of 0.5-1 mg. For each of  
144 the first three types of pollen species (populus tremuloides, populus deltoides and ragweed pollen),  
145 three samples in total were investigated, and each sample was studied under isothermal conditions  
146 at 5, 25 and 37 °C. For each of the other three types of pollen species (corn, pecan and paper  
147 mulberry pollen), experiments were carried out at 15 °C instead of 5 °C, because the instrument  
148 could only be cooled down to 15 °C due to a technical problem after we finished experiments for  
149 the first three pollen species.



150

151 **Figure 1.** Change of RH (black curve, left y-axis) and normalized sample mass (blue curve, right  
152 y-axis) with time for a typical experiment in which hygroscopic growth of pollen grains was  
153 measured. In this figure a dataset for paper mulberry pollen at 25 °C is plotted as an example.  
154

155 For the first sample, at each temperature the sample was first dried at 0% RH (the actual  
156 RH was measured to be <1%); after that, RH was increased stepwise to 95% with an increment of  
157 5% per step and then switched back to <1% to dry the sample again. At each RH, the sample was  
158 equilibrated with the environment (i.e. until the sample mass became stable) before RH was  
159 changed to the next value, and the sample mass was considered to be stabilized when the mass  
160 change was <0.05% within 30 min. Such a measurement at one temperature could take several  
161 days. In order to reduce experimental time, the second and third samples were investigated in a  
162 similar way as the first sample, except that RH was increased stepwise to 90% with an increment  
163 of 10% per step. A typical experimental dataset is displayed in Figure 1 as an example to illustrate  
164 the change of RH and normalized sample mass with experimental time.

### 165 **3 Results and discussion**

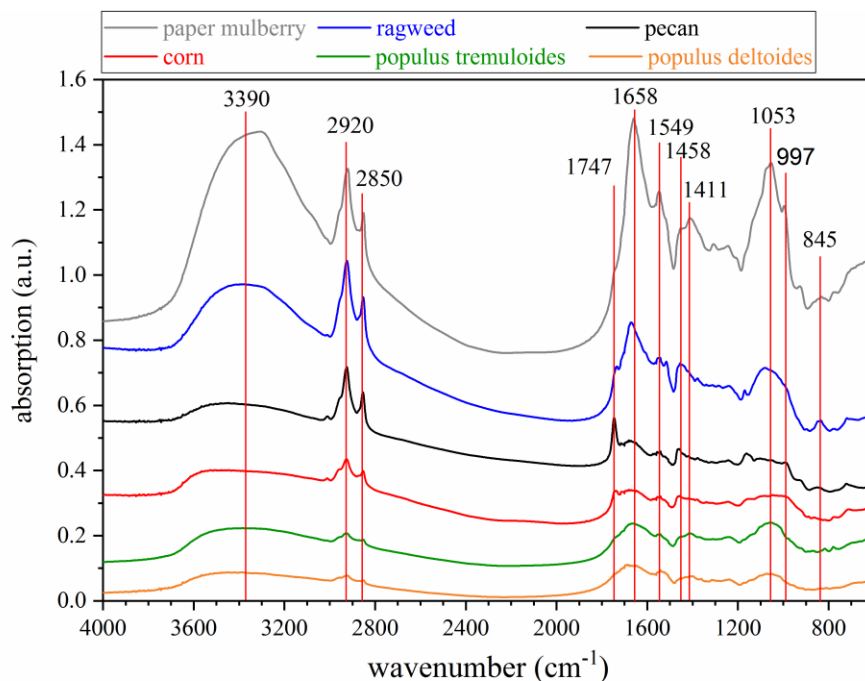
#### 166 **3.1 FTIR characterization of pollen samples**

##### 167 **3.1.1 Infrared spectra of dry pollen samples**

168 Figure 2 shows the transmission FTIR spectra of the six pollen species investigated in our  
169 work, and peak assignments can be found in Table 1. A broad band in the range of 3600-3000 cm<sup>-1</sup>,  
170 attributed to O-H stretching vibration (Stuart, 2004; Pummer et al., 2013), and two sharp peaks at  
171 2920 and 2850 cm<sup>-1</sup>, attributed to C-H stretching (Eliason et al., 2003; Stuart, 2004; Pummer et al.,  
172 2013), were observed for all the pollen species. The two peaks at 1747 and 1658 cm<sup>-1</sup> were  
173 assigned to alkyl ester carbonyls (Pappas et al., 2003; Najera et al., 2009; Pummer et al., 2013),



174 and the two peaks at 1549 and 1458  $\text{cm}^{-1}$  (1411  $\text{cm}^{-1}$  for paper mulberry pollen) were assigned to  
 175 C=C stretching and H-C-H deformation (Stuart, 2004; Pummer et al., 2013). In addition, the three  
 176 peaks at 1053, 997 and 845  $\text{cm}^{-1}$  were assigned to C-O stretching, C-C stretching, and C-H out-of-  
 177 plane bending, respectively (Stuart, 2004; Najera et al., 2009; Pummer et al., 2013).



178  
 179 **Figure 2.** Transmission FTIR spectra of six pollen species investigated in this work.

180  
 181 OH groups and C-H groups in organic compounds are generally considered to be  
 182 hydrophilic and hydrophobic, and one may expect that the amount of OH groups (relative to that  
 183 of C-H groups) that organic samples contain may affect their hygroscopicity. For example, it was  
 184 found in many previous studies (Eliason et al., 2003; Asad et al., 2004; Hung et al., 2005; Najera  
 185 et al., 2009) that heterogeneous reactions of organic materials with  $\text{O}_3$  and OH radicals would  
 186 increase the IR absorption intensity for the O-H stretching mode and decrease the IR absorption  
 187 intensity for the C-H stretching mode, meanwhile leading to the enhancement in their  
 188 hygroscopicity. Therefore, in this work we use the intensity ratio of the O-H stretching vibration

189 band (3000-3600  $\text{cm}^{-1}$ ) to the C-H stretching mode (2920  $\text{cm}^{-1}$ ) to qualitatively represent the  
 190 amount of OH groups pollen samples contain. As shown in Figure 2, the six pollen species  
 191 examined in our work can be roughly classified into two catalogues: 1) for populus deltoides,  
 192 populus tremuloides and paper mulberry pollen, the O-H stretching vibration band is more  
 193 intensive than the C-H stretching mode, indicating that they contain relatively high levels of OH  
 194 groups; 2) for ragweed, pecan and corn pollen, the O-H stretching vibration band is less intensive  
 195 than the C-H stretching mode, indicating that they contain relatively low levels of OH groups. The  
 196 relation between the amount of OH groups that pollen species contain and their hygroscopicity  
 197 will be further discussed in Section 3.3.

198

199 **Table 1.** Vibrational mode assignment for six pollen species investigated in this work.

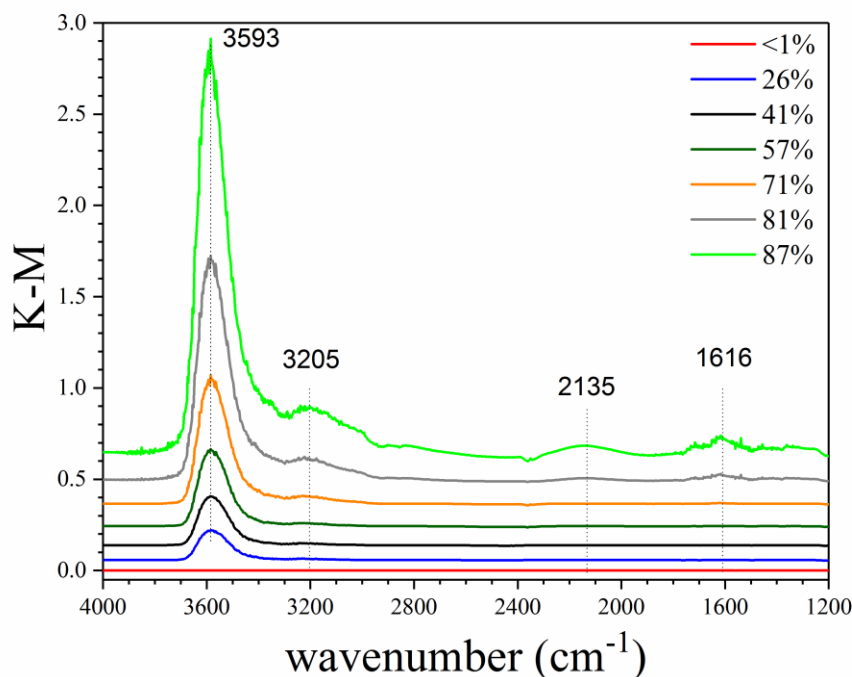
wavenumber ( $\text{cm}^{-1}$ )	vibrational mode
3600-3000	O-H stretching
2920 and 2820	C-H stretching
1747 and 1658	alkyl ester carbonyls
1549	C=C stretching
1458 and 1411	H-C-H deformation
1053	C-O stretching
997	C-C stretching
845	C-H out-of-plane bending

200

### 201 3.1.2 Infrared spectra of pollen samples at different RH

202 In-situ DRIFTS was employed to explore adsorption of water by pollen grains. Typical  
 203 spectra of populus deltoides pollen as a function of RH up to 87%, relative to that at <1% RH,  
 204 are displayed in Figure 3. DRIFTS spectra of other pollen samples at different RH can be found in  
 205 Figures S1-S5 in the supplement, and are very similar to those for populus deltoides pollen. As

206 evident from Figure 3, several IR peaks (e.g., 3593, 3205, 2135, and 1616  $\text{cm}^{-1}$ ) appeared in the  
 207 spectra at elevated RH, when compared with that at <1% RH, and their intensities increased with  
 208 increasing RH. The peaks at 3205, 2135 and 1616  $\text{cm}^{-1}$  can be assigned to the stretching,  
 209 association and bending modes of adsorbed water (Goodman et al., 2001; Schuttlefield et al.,  
 210 2007a; Ma et al., 2010; Hatch et al., 2011; Song and Boily, 2013; Yeşilbaş and Boily, 2016; Joshi  
 211 et al., 2017; Ibrahim et al., 2018).



212  
 213 **Figure 3.** In-situ DRIFTS spectra of populus deltoides pollen as a function of RH (<1, 26, 41, 57,  
 214 71, 81 and 87%) at 25 °C.

215  
 216 The peak at  $\sim 3600 \text{ cm}^{-1}$  was the most intensive one observed in the spectra, as shown in  
 217 Figure 3. For comparison, the IR peaks assigned to the stretching mode of adsorbed water on  
 218 mineral dust and NaCl appeared at lower wavenumbers, typically at around or lower than 3400  
 219  $\text{cm}^{-1}$  (Schuttlefield et al., 2007a; Ma et al., 2010; Tang et al., 2016; Ibrahim et al., 2018). As a  
 220 result, the peak at  $\sim 3600 \text{ cm}^{-1}$  may be assigned to the asymmetric stretching mode of water which

221 interacted with OH groups in pollen samples (Iwamoto et al., 2003). These results imply that water  
 222 adsorption by pollen samples **could be** mainly contributed by OH groups of organic compounds  
 223 they contained; **in addition, other factors, such as porosity and internal structure, may also be**  
 224 **important for hygroscopic properties of pollen grains.** The intensities of IR peaks at  $\sim 3600\text{ cm}^{-1}$   
 225 were used to represent the amount of water adsorbed by pollen samples. Table 2 summarizes  
 226 integrated areas of IR peaks at  $3600\text{ cm}^{-1}$  as a function of RH for the six pollen species examined  
 227 in our work, suggesting that the amount of adsorbed water by pollen samples increased with RH.

228  
 229 **Table 2.** Integrated areas of IR peaks (at  $\sim 3600\text{ cm}^{-1}$ ) of adsorbed water as a function of RH for  
 230 the six pollen species investigated in this work. Wavenumber ranges used for integration are 3750-  
 231  $3300\text{ cm}^{-1}$  for populus deltoides pollen, 3750-3350  $\text{cm}^{-1}$  for populus tremuloides pollen, 3750-  
 232  $3400\text{ cm}^{-1}$  for ragweed pollen, 3750-3500  $\text{cm}^{-1}$  for corn pollen, 3750-3450  $\text{cm}^{-1}$  for pecan pollen,  
 233 and 3750-3300  $\text{cm}^{-1}$  for paper mulberry pollen.

RH (%)	peak area	RH (%)	peak area	RH (%)	peak area
populus deltoides		populus tremuloides		ragweed	
0	0	0	0	0	0
26	22.7	24	5.5	26	10.1
41	36.9	41	16.4	42	18.9
57	57.4	56	35.4	50	24.5
71	93.6	70	66.5	56	30.2
79	137.6	78	91.2	69	49.7
81	164.7	87	156.9	88	104.6
87	293.1				
corn		pecan		paper mulberry	
0	0	0	0	0	0
26	10.0	26	8.6	26	10.2
42	21.5	43	16.9	43	17.7
58	41.9	58	29.5	51	23.1

73	87.5	73	60.0	59	29.8
89	222.2	89	338.9	71	46.7
				86	105.1

234

## 235 3.2 Mass hygroscopic growth

### 236 3.2.1 Hygroscopicity parameterizations

237 The single hygroscopicity parameter,  $\kappa$ , is widely used to describe the hygroscopicity of  
238 aerosol particles under both subsaturation and supersaturation (Petters and Kreidenweis, 2007).  
239 When the Kelvin effect is negligible (this is valid for pollen grains which are typically  $>1 \mu\text{m}$ ), the  
240 dependence of diameter-based growth factor (GF) on RH can be linked to  $\kappa$  via Eq. (1) (Petters  
241 and Kreidenweis, 2007; Tang et al., 2016):

$$242 \quad RH = \frac{GF^3 - 1}{GF^3 - 1 + \kappa} \quad (1)$$

243 If we further assume that the particle is spherical, Eq. (1) can be transformed to Eq. (2):

$$244 \quad \frac{1}{RH} = 1 + \frac{\kappa}{GF^3 - 1} = 1 + \frac{\kappa}{\frac{V}{V_0} - 1} = 1 + \kappa \frac{V_0}{V - V_0} = 1 + \kappa \frac{V_0}{V_w} \quad (2)$$

245 where  $V$ ,  $V_0$  and  $V_w$  are the volumes of the particle at the given RH, the dry particle and water  
246 associated with the particle at the given RH. In order for Eq. (2) to be valid, it is also assumed that  
247 at a given RH,  $V$  is equal to the sum of  $V_0$  and  $V_w$ . Eq. (2) can be further transformed to Eqs. (3-4):

$$248 \quad \frac{1}{RH} = 1 + \kappa \frac{\rho_w m_0}{\rho_p m_w} \quad (3)$$

$$249 \quad \frac{m_w}{m_0} = \kappa \cdot \frac{\rho_w}{\rho_p} / \left( \frac{1}{RH} - 1 \right) \quad (4)$$

250 where  $\rho_w$  and  $\rho_p$  are the density of water and the dry particle, and  $m_0$  and  $m_w$  are the mass of the  
251 dry particle and water associated with the particle at the given RH. Since the particle mass,  $m$ , is  
252 equal to the sum of  $m_0$  and  $m_w$ , Eq. (5) can be derived from Eq. (4):

253 
$$\frac{m}{m_0} = 1 + \kappa \frac{\rho_w}{\rho_p} / \left( \frac{1}{RH} - 1 \right) \quad (5)$$

254 Using an electrodynamic balance, Pope and co-workers (Pope, 2010; Griffiths et al., 2012)  
255 measured hygroscopic growth of eight types of pollen grains, and found that their mass change  
256 with RH can be approximated by Eq. (5). It should be noted that the original equation derived by  
257 Pope and co-workers (Pope, 2010; Griffiths et al., 2012) has a different format from but is  
258 essentially equivalent to Eq. (5). Eq. (5) relates mass growth experimentally measured in our work  
259 to the single hygroscopicity parameter ( $\kappa$ ), which has been widely used in atmospheric science to  
260 describe hygroscopic properties of aerosol particles under subsaturation as well as their CCN  
261 activities under supersaturation; nevertheless, a few assumptions are needed to derive Eq. (5), as  
262 discussed.

263 The Freundlich adsorption isotherm is another widely used equation to describe the change  
264 of sample mass with RH due to water uptake (Atkins, 1998; Skopp, 2009; Hatch et al., 2011; Tang  
265 et al., 2016):

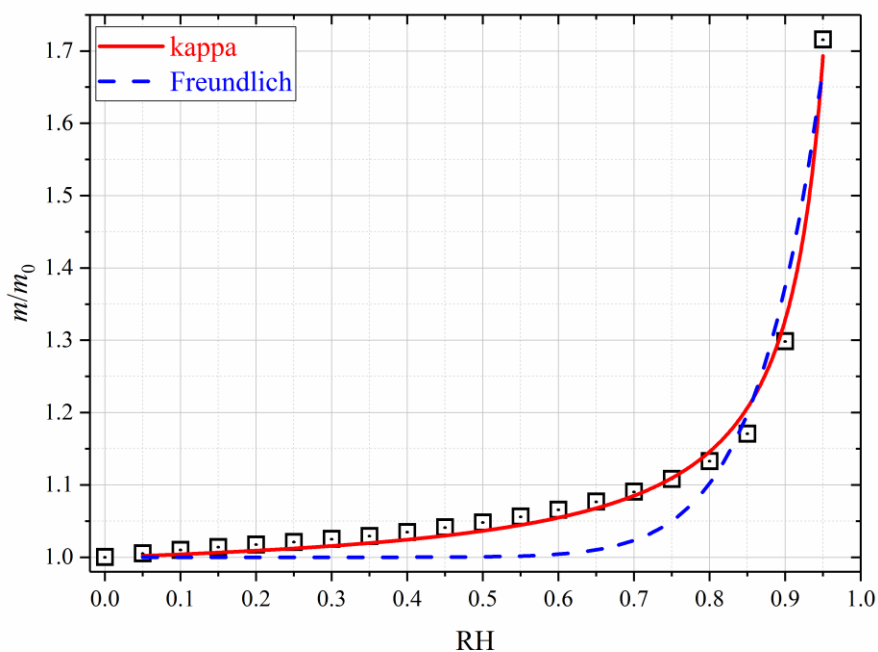
266 
$$\frac{m}{m_0} = 1 + A_f \cdot \sqrt[B_f]{RH} \quad (6)$$

267 where  $A_f$  and  $B_f$  are empirical Freundlich constants related to the adsorption capacity and strength.  
268 One advantage of the Freundlich adsorption isotherm is that it provides a direct relationship  
269 between RH and mass growth which was experimentally measured in our work, without any  
270 additional assumptions. In addition, the BET (Brunauer-Emmett-Teller) adsorption isotherm is  
271 also widely used to describe water adsorption by insoluble solid particles (Brunauer et al., 1938;  
272 Goodman et al., 2001; Henson, 2007; Ma et al., 2010; Tang et al., 2016; Joshi et al., 2017). While  
273 the BET adsorption isotherm typically works well for water adsorption of a few monolayers, the  
274 mass of adsorbed water, as shown in Section 3.2.2, can reach up to 50% of the dry pollen mass at  
275 high RH; therefore, in this work we did not attempt to use the BET adsorption isotherm to describe

276 water adsorption by pollen grains. Another reason that we did not attempt to use the BET  
277 adsorption isotherm is that the BET adsorption isotherm is mathematically more complex and  
278 requires the BET surface area to be known.

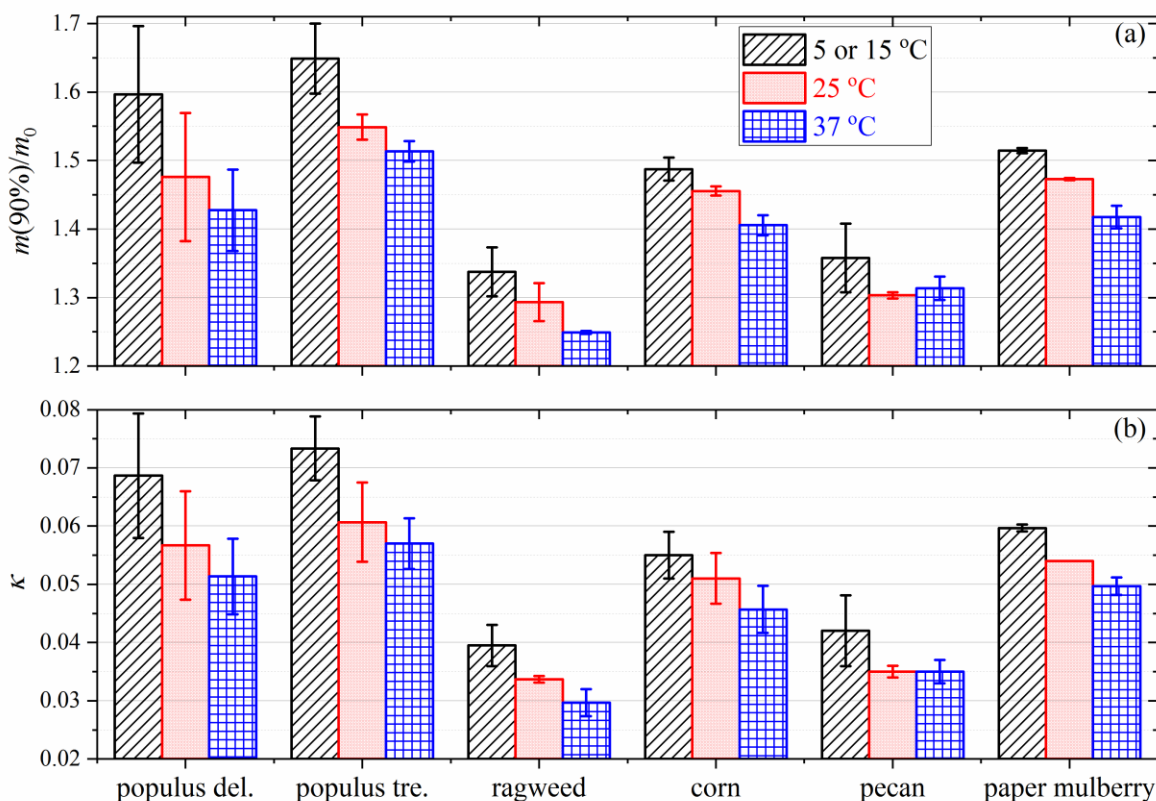
### 279 3.2.2 Mass hygroscopic growth at room temperature

280 Figure 4 displays the sample mass (normalized to that at 0% RH) as a function of RH for  
281 pecan pollen at 25 °C. Significant increase in sample mass was observed at elevated RH due to  
282 uptake of water. Compared to that at 0% RH, the sample mass increased by  $(2.3\pm 0.3)\%$  at 30%  
283 RH,  $(6.4\pm 0.2)\%$  at 60% RH,  $(30.3\pm 0.4)\%$  at 90% RH, and up to  $\sim 72\%$  at 95% RH. As shown by  
284 the data compiled in Tables S1-S3 in the supplement, substantial increases in sample mass were  
285 also observed for the other five types of pollen species at 25 °C (as well as 5 and 37 °C).



286  
287 **Figure 4.** Measured change of sample mass (normalized to that at dry conditions, i.e.  $m/m_0$ ) of  
288 pecan pollen as a function of RH (0-0.95) at 25 °C. The experimental data are fitted with the  
289 modified  $\kappa$ -Köhler equation (solid red curve) and the Freundlich adsorption isotherm (dashed blue  
290 curve).

291  
 292 Hygroscopic properties exhibited considerable variations among different pollen species.  
 293 Figure 5a compares the measured ratios of sample mass at 90% RH to that at 0% RH,  $m(90\%)/m_0$ ,  
 294 for the six pollen species investigated in this work. We specifically discuss mass changes of pollen  
 295 grains at 90% RH (relative to that at 0% RH) because aerosol hygroscopic growth at 90% RH was  
 296 widely reported by laboratory and field studies (Kreidenweis and Asa-Awuku, 2014). As shown  
 297 in Figure 5a,  $m(90\%)/m_0$  determined at 25 °C ranged from  $1.293\pm 0.028$  (ragweed pollen) to  
 298  $1.476\pm 0.094$  (populus deltoides pollen), i.e. the amount of water adsorbed/absorbed by the six  
 299 different pollen species at 90% RH varied between ~30% to ~50% of the dry mass.



300  
 301 **Figure 5.** Measured ratios of sample mass at 90% RH to that at 0% RH (a) and derived  $\kappa$  values  
 302 (b) for six pollen species at different temperatures. The lowest temperatures were 5 °C for populus



303 deltooides (populus del.), populus tremuloides (populus tre.) and ragweed pollen, and 15 °C for corn,  
304 pecan and paper mulberry pollen.

305  
306 As shown in Figure 4, the increase of pecan pollen mass with RH at 25 °C could be  
307 satisfactorily described by the modified  $\kappa$ -Köhler equation for the entire RH range (up to 95%).  
308 On the contrary, the Freundlich adsorption isotherm significantly underestimated the sample mass  
309 at low RH, although it represented the experimental data at high RH reasonably well. In addition,  
310 we found that the modified  $\kappa$ -Köhler equation could also approximate the dependence of sample  
311 mass on RH for all the six types of pollen species investigated in this work at different temperatures.  
312 If we use Eq. (5) to fit  $m/m_0$  against RH,  $\kappa \cdot \rho_w / \rho_p$  can be derived. The bulk densities of dry pollen  
313 grains were found to vary with species but typically fall into the range of 0.5-2 g cm<sup>-3</sup> (Harrington  
314 and Metzger, 1963; Hirose and Osada, 2016), and for simplicity  $\rho_p$  was assumed to be 1 g cm<sup>-3</sup> in  
315 this work (i.e.  $\rho_w / \rho_p$  is equal to 1). With the assumptions on dry particle density and also particle  
316 sphericity,  $\kappa$  could then be derived from the measured RH-dependent sample mass at a given  
317 temperature.

318 Table 3 summarizes the average  $\kappa$  values at different temperatures for the six pollen species  
319 investigated in this work. At 25 °C, the  $\kappa$  values were found to increase from 0.034±0.001 for  
320 ragweed pollen to 0.061±0.007 for populus tremuloides pollen, varied by almost a factor of 2. The  
321  $\kappa$  values measured by Pope and co-workers (Pope, 2010; Griffiths et al., 2012) were approximately  
322 in the range of 0.05-0.11 (assuming that  $\rho_w / \rho_p$  is equal to 1), in reasonably good agreement with  
323 these reported in our work. It should be noted that in order to convert the measured mass growth  
324 to diameter growth and  $\kappa$  values, one key assumption is particle sphericity; nevertheless, pollen  
325 grains are known to be non-spherical and porous, and therefore our derived  $\kappa$  values might be

326 smaller than the actual values. For example, although the mass increase was substantial (around  
 327 30-50 % at 90% RH) for the six pollen species examined, their  $\kappa$  values at 25 °C were derived to  
 328 be in the range of 0.034-0.061, significantly smaller than those (0.1-0.2) for typical secondary  
 329 organic aerosols produced in smog chamber studies (Petters and Kreidenweis, 2007; Kreidenweis  
 330 and Asa-Awuku, 2014).

331  
 332 **Table 3.** Single hygroscopicity parameters ( $\kappa$ ) derived in this work for the six pollen species at  
 333 different temperatures. All the errors given in this work are standard deviations.

pollen type	$T$ (°C)	sample 1	sample 2	sample 3	average
populus	5	0.071±0.001	0.078±0.001	0.057±0.002	0.069±0.011
deltoides	25	0.054±0.001	0.067±0.002	0.049±0.002	0.057±0.009
	37	0.058±0.002	0.051±0.001	0.045±0.002	0.051±0.007
populus	5	0.068±0.001	0.073±0.001	0.079±0.001	0.073±0.006
tremuloides	25	0.053±0.002	0.063±0.002	0.066±0.002	0.061±0.007
	37	0.052±0.002	0.059±0.002	0.060±0.002	0.057±0.004
ragweed	5	0.042±0.001	0.037±0.002	--	0.040±0.004
	25	0.033±0.002	0.034±0.003	0.034±0.002	0.034±0.001
	37	0.027±0.001	0.031±0.002	0.031±0.002	0.030±0.002
corn	15	0.051±0.001	0.059±0.002	0.055±0.002	0.055±0.004
	25	0.046±0.002	0.053±0.002	0.054±0.002	0.051±0.004
	37	0.041±0.002	0.048±0.002	0.048±0.002	0.046±0.004
pecan	15	0.049±0.001	0.038±0.001	0.039±0.001	0.042±0.006
	25	0.036±0.001	0.034±0.001	0.035±0.001	0.035±0.001
	37	0.033±0.001	0.035±0.002	0.037±0.001	0.035±0.002
paper	15	0.059±0.002	0.060±0.002	0.060±0.002	0.060±0.001
mulberry	25	0.054±0.001	0.054±0.001	0.054±0.001	0.054±0.001
	37	0.048±0.002	0.050±0.002	0.051±0.002	0.050±0.002

334

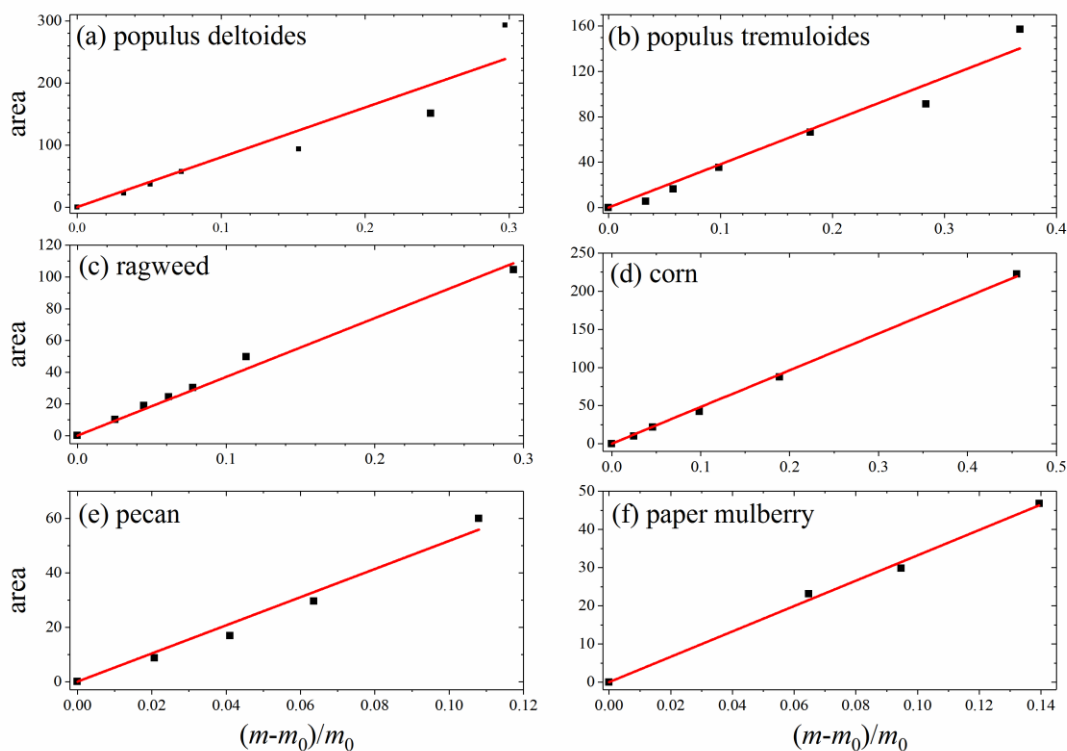
### 335 **3.3 Discussion**

#### 336 **3.3.1 Reconciliation between IR and VSA results**

337 Our in-situ DRIFTS measurements, as discussed in Section 3.1.2, suggested that water  
338 uptake by pollen samples was mainly contributed by OH groups of organic compounds they  
339 contained; therefore, one may expect that pollen species which contain higher levels of OH groups  
340 would exhibit higher hygroscopicity. Transmission FTIR characterization of pollen species  
341 (Section 3.1.1) showed that populus deltoides, populus tremuloides and paper mulberry pollen  
342 contained relatively high levels of OH groups, and indeed their hygroscopicity ( $\kappa$ : 0.053-0.054 at  
343 25 °C) was higher than the other three pollen species, as shown in Figure 5 and Table 3. For  
344 comparison, ragweed and pecan pollen contained relatively low levels of OH groups and  
345 correspondingly exhibited lower hygroscopicity ( $\kappa$ : 0.033-0.036 at 25 °C). Corn pollen appeared  
346 to be an exception: it contained relatively low levels of OH group but displayed medium  
347 hygroscopicity ( $\kappa$ : ~0.046 at 25 °C). As a result, our results may imply that in addition to chemical  
348 composition, other physicochemical properties, such as porosity and internal structure of pollen  
349 grains, could also play an important role in determining the hygroscopicity of pollen species. One  
350 clue came from environmental scanning electron microscopy observations (Pope, 2010), revealing  
351 that pollen grains started to swell internally before significant water uptake on the surface took  
352 place.

353 In our work two complementary techniques were employed to explore hygroscopic  
354 properties of pollen species. VSA measured the amount of water absorbed/adsorbed by pollen  
355 grains as a function of RH in a quantitative manner, whereas the intensities of IR peaks of adsorbed  
356 water at different RH, as characterized by DRIFTS, can be used semi-quantitatively to represent  
357 the amount of water associated with particles (Goodman et al., 2001; Schuttlefield et al., 2007b;

358 Ma et al., 2010; Yeşilbaş and Boily, 2016; Joshi et al., 2017; Ibrahim et al., 2018). We compare  
 359 our VSA results (i.e. the relative mass change due to water uptake) to the DRIFTS results (i.e.  
 360 integrated area of IR peaks at  $\sim 3600\text{ cm}^{-1}$ ). As shown in Figure 6, good correlations between VSA  
 361 and DRIFTS results are found for all the six pollen species, suggesting that DRIFTS can be used  
 362 to represent the amount of adsorbed water, at least in a semi-quantitative manner.



363  
 364 **Figure 6.** Integrated areas of IR peaks at  $\sim 3600\text{ cm}^{-1}$  versus relative mass increase due to water  
 365 uptake,  $(m-m_0)/m_0$ , for six pollen species: (a) populus deltoides; (b) populus tremuloides; (c)  
 366 ragweed; (d) corn; (e) pecan; (f) paper mulberry.

367

### 368 3.3.2 Effect of temperature

369 Figure 5a shows the comparison of the measured ratios of sample mass at 90% RH to that  
 370 at 0% RH,  $m(90\%)/m_0$ , at different temperatures for the six pollen species. It can be concluded

371 from Figure 5a that except for pecan pollen for which a small increase in  $m(90\%)/m_0$  occurred  
372 when temperature increased from 25 to 37 °C, increase in temperature would lead to small but  
373 nevertheless significant decrease in  $m(90\%)/m_0$ . For example,  $m(90\%)/m_0$  decreased from  
374  $1.597\pm 0.100$  at 5 °C to  $1.476\pm 0.094$  at 25 °C and to  $1.427\pm 0.060$  at 37 °C for populus deltoides  
375 pollen, and from  $1.338\pm 0.036$  at 5 °C to  $1.293\pm 0.028$  at 25 °C and to  $1.249\pm 0.002$  at 37 °C for  
376 ragweed pollen.

377 We further derived  $\kappa$  values at different temperatures for the six pollen species, and the  
378 results are plotted in Figure 5b and summarized in Table 3. Increase in temperature would lead to  
379 decrease in  $\kappa$  values, except for pecan pollen. For example,  $\kappa$  decreased from  $0.073\pm 0.006$  at 5 °C  
380 to  $0.057\pm 0.004$  at 37 °C for populus tremuloides pollen, and decreased from  $0.060\pm 0.001$  at 15 °C  
381 to  $0.050\pm 0.002$  at 37 °C for paper mulberry pollen.

## 382 **4 Conclusion and implications**

383 Pollen grains are one of the most abundant types of primary biological aerosol particles in  
384 the troposphere and play important roles in many aspects of the Earth system. Hygroscopicity is  
385 among the most important physicochemical properties of pollen grains and largely affect their  
386 environmental, health and climatic impacts. However, our knowledge in their hygroscopicity is  
387 still quite limited, and especially the temperature effect has been rarely explored.

388 In this work we investigated hygroscopic properties of six types of pollen species as a  
389 function of RH (up to 95%) at 5 (or 15), 25 and 37 °C. Substantial increase in pollen mass was  
390 observed at elevated RH due to water uptake for all the six pollen species. Therefore, change in  
391 the mass of pollen grains and their aerodynamic properties at different RH should be taken into  
392 account to better understand their transport and deposition in the troposphere. It was found that the  
393 mass hygroscopic growth of pollen grains can be well approximated by the modified  $\kappa$ -Köhler

394 **equation.** The derived  $\kappa$  values at 25 °C ranged from  $0.034\pm 0.001$  to  $0.061\pm 0.007$ , varying with  
395 pollen species. DRIFTS measurements indicated that water adsorption by pollen species were  
396 mainly contributed by OH groups of organic compounds contained by pollen grains, and indeed  
397 pollen species that contained lower levels of OH groups (relative to C-H groups, as determined  
398 using transmission FTIR) showed lower hygroscopicity. One exception was corn pollen which  
399 contained low levels of OH group but exhibited medium hygroscopicity, suggesting that in  
400 addition to chemical composition, other physicochemical properties, such as porosity and internal  
401 structure, might also play an important role in determining the hygroscopicity of pollen grains.  
402 Due to their moderate hygroscopicity as well as large sizes, pollen grains can thus act as efficient  
403 giant CCN which may have significant impacts on cloud and precipitation (Johnson, 1982;  
404 Feingold et al., 1999; Yin et al., 2000; Posselt and Lohmann, 2008). It is worth noting that only  
405 six different pollen species were examined in our work, and hygroscopic properties of other pollen  
406 species commonly found in the troposphere should be further investigated.

407 The effect of temperature on the hygroscopicity of pollen grains was systematically  
408 investigated in this work. Increase in temperature (from 5 or 15 °C to 25 and 37 °C), a range  
409 covering chilling temperature to physiological temperature, led to small but detectable decrease in  
410 pollen hygroscopicity. For example,  $\kappa$  values were found to decrease from  $0.073\pm 0.006$  at 5 °C to  
411  $0.061\pm 0.007$  at 25 °C and to  $0.057\pm 0.004$  at 37 °C for populus tremuloides pollen, and decrease  
412 from  $0.060\pm 0.001$  at 15 °C to  $0.054\pm 0.001$  at 25 °C to  $0.050\pm 0.002$  at 37 °C for paper mulberry  
413 pollen. Our measurements at 37 °C (physiological temperature) provide very valuable parameters  
414 which can be used in numerical models to better understand the transport and deposition of pollen  
415 particles in the respiratory system and thus their impacts on human health (Yeh et al., 1996; Broday  
416 and Georgopoulos, 2001; Park and Wexler, 2008; Lambert et al., 2011; Longest and Holbrook,

417 2012; Tong et al., 2014). Nevertheless, it should be noted that due to the short residence time in  
418 the respiratory system, pollen grains and other inhaled particles in general, may not reach  
419 equilibrium with water vapor in the respiratory tract.

420 Due to technical challenges, the lowest temperature we could reach in this work was 5 °C,  
421 in the range of normal chilling temperatures for vegetative species and also in the expected  
422 temperature range at the altitudes of 0.5-2.0 km to which pollen grains can be easily transported.  
423 Temperatures in the upper troposphere can be as low as below -70 °C, and it is yet to be explored  
424 whether further decrease in temperature to far below 0 °C will lead to large increase in pollen  
425 hygroscopicity. As a result, experimental measurements of pollen hygroscopicity at lower  
426 temperatures are warranted and would significantly help better understand the transport of pollen  
427 grains in the troposphere. Since water vapor has to be adsorbed or condensed on ice nucleating  
428 particles before heterogeneous ice nucleation can take place (Laaksonen et al., 2016), knowledge  
429 in hygroscopicity and water uptake at temperatures below 0 °C would provide fundamental insights  
430 into atmospheric ice nucleation, in which pollen grains may play an important role (Pratt et al.,  
431 2009; Prenni et al., 2009; Hoose et al., 2010; Pöschl et al., 2010; Murray et al., 2012; Creamean et  
432 al., 2013; Tang et al., 2018).

### 433 **Author contribution**

434 MT, QM and YJL designed the research; WG, CZ, SL and XY did the measurements; MT,  
435 QM, YJL and RJH analyzed the results; MT, QM, YJL and RJH wrote the manuscript with  
436 contribution from all the co-authors.

### 437 **Acknowledgment**

438 This work was funded by National Natural Science Foundation of China (91644106,  
439 91744204 and 91644219), Chinese Academy of Sciences (132744KYSB20160036), Science and

440 Technology Development Fund of Macau (016/2017/A1), and State Key Laboratory of Organic  
441 Geochemistry (SKLOG2016-A05). Mingjin Tang would like to thank the CAS Pioneer Hundred  
442 Talents program for providing a starting grant.

## 443 Reference

- 444 Ariya, P. A., Sun, J., Eltouny, N. A., Hudson, E. D., Hayes, C. T., and Kos, G.: Physical and chemical  
445 characterization of bioaerosols – Implications for nucleation processes, *Int. Rev. Phys. Chem.*, 28, 1-32, 2009.
- 446 Asad, A., Mmereki, B. T., and Donaldson, D. J.: Enhanced uptake of water by oxidatively processed oleic acid,  
447 *Atmos. Chem. Phys.*, 4, 2083-2089, 2004.
- 448 Atkins, P. W.: *Physical Chemistry (Sixth Edition)*, Oxford University Press, Oxford, UK, 1998.
- 449 Bauer, H., Giebl, H., Hitznerberger, R., Kasper-Giebl, A., Reischl, G., Zibuschka, F., and Puxbaum, H.: Airborne  
450 bacteria as cloud condensation nuclei, *J. Geophys. Res.-Atmos.*, 108, 4658, doi: 4610.1029/2003JD003545, 2003.
- 451 Broday, D. M., and Georgopoulos, P. G.: Growth and Deposition of Hygroscopic Particulate Matter in the Human  
452 Lungs, *Aerosol Sci. Technol.*, 34, 144-159, 2001.
- 453 Brunauer, S., Emmett, P. H., and Teller, E.: Adsorption of Gases in Multimolecular Layers, *J. Am. Chem. Soc.*, 60,  
454 309-319, 1938.
- 455 Bunderson, L. D., and Levetin, E.: Hygroscopic weight gain of pollen grains from *Juniperus* species, *Int. J.*  
456 *Biometeorol.*, 59, 533-540, 2015.
- 457 Creamean, J. M., Suski, K. J., Rosenfeld, D., Cazorla, A., DeMott, P. J., Sullivan, R. C., White, A. B., Ralph, F. M.,  
458 Minnis, P., Comstock, J. M., Tomlinson, J. M., and Prather, K. A.: Dust and Biological Aerosols from the Sahara  
459 and Asia Influence Precipitation in the Western U.S, *Science*, 339, 1572-1578, 2013.
- 460 Deguillaume, L., Leriche, M., Amato, P., Ariya, P. A., Delort, A. M., Poschl, U., Chaumerliac, N., Bauer, H.,  
461 Flossmann, A. I., and Morris, C. E.: Microbiology and atmospheric processes: chemical interactions of primary  
462 biological aerosols, *Biogeosciences*, 5, 1073-1084, 2008.
- 463 Després, V. R., Huffman, J. A., Burrows, S. M., Hoose, C., Safatov, A. S., Buryak, G., Fröhlich-Nowoisky, J.,  
464 Elbert, W., Andreae, M. O., Pöschl, U., and Jaenicke, R.: Primary biological aerosol particles in the atmosphere: a  
465 review, *Tellus B*, 64, 15598, 2012.
- 466 Diehl, K., Quick, C., Matthias-Maser, S., Mitra, S. K., and Jaenicke, R.: The ice nucleating ability of pollen - Part I:  
467 Laboratory studies in deposition and condensation freezing modes, *Atmos. Res.*, 58, 75-87, 2001.
- 468 Douwes, J., Thorne, P., Pearce, N., and Heederik, D.: Bioaerosol health effects and exposure assessment: Progress  
469 and prospects, *Ann. Occup. Hyg.*, 47, 187-200, 2003.
- 470 Eliason, T. L., Aloisio, S., Donaldson, D. J., Cziczko, D. J., and Vaida, V.: Processing of unsaturated organic acid  
471 films and aerosols by ozone, *Atmos. Environ.*, 37, 2207-2219, 2003.
- 472 Estillore, A. D., Trueblood, J. V., and Grassian, V. H.: Atmospheric chemistry of bioaerosols: heterogeneous and  
473 multiphase reactions with atmospheric oxidants and other trace gases, *Chem. Sci.*, 7, 6604-6616, 2016.
- 474 Feingold, G., Cotton, W. R., Kreidenweis, S. M., and Davis, J. T.: The Impact of Giant Cloud Condensation Nuclei  
475 on Drizzle Formation in Stratocumulus: Implications for Cloud Radiative Properties, *J. Atmos. Sci.*, 56, 4100-4117,  
476 1999.
- 477 Fröhlich-Nowoisky, J., Kampf, C. J., Weber, B., Huffman, J. A., Pöhlker, C., Andreae, M. O., Lang-Yona, N.,  
478 Burrows, S. M., Gunthe, S. S., Elbert, W., Su, H., Hoor, P., Thines, E., Hoffmann, T., Després, V. R., and Pöschl,  
479 U.: Bioaerosols in the Earth system: Climate, health, and ecosystem interactions, *Atmos. Res.*, 182, 346-376, 2016.
- 480 Franc, G. D., and DeMott, P. J.: Cloud activation characteristics of airborne *Erwinia carotovora* cells, *J. Appl. Met.*,  
481 37, 1293-1300, 1998.
- 482 Georgakopoulos, D. G., Després, V., Fröhlich-Nowoisky, J., Psenner, R., Ariya, P. A., Pósfai, M., Ahern, H. E.,  
483 Moffett, B. F., and Hill, T. C. J.: Microbiology and atmospheric processes: biological, physical and chemical  
484 characterization of aerosol particles, *Biogeosciences*, 6, 721-737, 2009.
- 485 Goodman, A. L., Bernard, E. T., and Grassian, V. H.: Spectroscopic Study of Nitric Acid and Water Adsorption on  
486 Oxide Particles: Enhanced Nitric Acid Uptake Kinetics in the Presence of Adsorbed Water, *J. Phys. Chem. A*, 105,  
487 6443-6457, 2001.
- 488 Griffiths, P. T., Borlace, J. S., Gallimore, P. J., Kalberer, M., Herzog, M., and Pope, F. D.: Hygroscopic growth and  
489 cloud activation of pollen: a laboratory and modelling study, *Atmos. Sci. Lett.*, 13, 289-295, 2012.



490 Gu, W. J., Li, Y. J., Zhu, J. X., Jia, X. H., Lin, Q. H., Zhang, G. H., Ding, X., Song, W., Bi, X. H., Wang, X. M., and  
491 Tang, M. J.: Investigation of water adsorption and hygroscopicity of atmospherically relevant particles using  
492 a commercial vapor sorption analyzer, *Atmos. Meas. Tech.*, 10, 3821-3832, 2017.

493 Guo, L. Y., Gu, W. J., Peng, C., Wang, W. G., Li, Y. J., Zong, T. M., Tang, Y. J., Wu, Z. J., Lin, Q. H., Ge, M. F.,  
494 Zhang, G. H., Hu, M., Bi, X. H., Wang, X. M., and Tang, M. J.: A comprehensive study of hygroscopic properties of  
495 calcium- and magnesium-containing salts: implication for hygroscopicity of mineral dust and sea salt aerosols,  
496 *Atmos. Chem. Phys. Discuss.*, 2018, 1-37, 10.5194/acp-2018-412, 2018.

497 Gute, E., and Abbatt, J. P. D.: Oxidative Processing Lowers the Ice Nucleation Activity of Birch and Alder Pollen,  
498 *Geophys. Res. Lett.*, 45, 1647-1653, 2018.

499 Harrington, J. B., and Metzger, K.: Ragweed Pollen Density, *Amer. J. Bot.*, 50, 532-539, 1963.

500 Hatch, C. D., Wiese, J. S., Crane, C. C., Harris, K. J., Kloss, H. G., and Baltrusaitis, J.: Water Adsorption on Clay  
501 Minerals As a Function of Relative Humidity: Application of BET and Freundlich Adsorption Models, *Langmuir*,  
502 28, 1790-1803, 2011.

503 Henson, B. F.: An adsorption model of insoluble particle activation: Application to black carbon, *J. Geophys. Res. -*  
504 *Atmos.*, 112, D24S16, doi: 10.1029/2007JD008549, 2007.

505 Hirose, Y., and Osada, K.: Terminal settling velocity and physical properties of pollen grains in still air,  
506 *Aerobiologia*, 32, 385-394, 2016.

507 Hoose, C., Kristjansson, J. E., and Burrows, S. M.: How important is biological ice nucleation in clouds on a global  
508 scale?, *Environ. Res. Lett.*, 5, 024009, 2010.

509 Hung, H. M., Katrib, Y., and Martin, S. T.: Products and mechanisms of the reaction of oleic acid with ozone and  
510 nitrate radical, *J. Phys. Chem. A*, 109, 4517-4530, 2005.

511 Ibrahim, S., Romanias, M. N., Alleman, L. Y., Zeineddine, M. N., Angeli, G. K., Trikalitis, P. N., and Thevenet, F.:  
512 Water Interaction with Mineral Dust Aerosol: Particle Size and Hygroscopic Properties of Dust, *ACS Earth and*  
513 *Space Chem.*, 2, 376-386, 2018.

514 International-Grains-Council: Grain Market Report GMR 495, 2019.

515 Iwamoto, R., Matsuda, T., Sasaki, T., and Kusanagi, H.: Basic interactions of water with organic compounds, *J.*  
516 *Phys. Chem. B*, 107, 7976-7980, 2003.

517 Jia, X. H., Gu, W. J., Li, Y. J., Cheng, P., Tang, Y. J., Guo, L. Y., Wang, X. M., and Tang, M. J.: Phase transitions  
518 and hygroscopic growth of  $Mg(ClO_4)_2$ ,  $NaClO_4$ , and  $NaClO_4 \cdot H_2O$ : implications for the stability of aqueous water  
519 in hyperarid environments on Mars and on Earth, *ACS Earth Space Chem.*, 2, 159-167, 2018.

520 Johnson, D. B.: The Role of Giant and Ultragiant Aerosol Particles in Warm Rain Initiation, *J. Atmos. Sci.*, 39, 448-  
521 460, 1982.

522 Joshi, N., Romanias, M. N., Riffault, V., and Thevenet, F.: Investigating water adsorption onto natural mineral dust  
523 particles: Linking DRIFTS experiments and BET theory, *Aeolian Res.*, 27, 35-45, 2017.

524 Ko, G., First, M. W., and Burge, H. A.: Influence of relative humidity on particle size and UV sensitivity of *Serratia*  
525 *marcescens* and *Mycobacterium bovis* BCG aerosols, *Tubercle and Lung Disease*, 80, 217-228, 2000.

526 Kreidenweis, S. M., and Asa-Awuku, A.: 5.13 - Aerosol Hygroscopicity: Particle Water Content and Its Role in  
527 Atmospheric Processes, in: *Treatise on Geochemistry (Second Edition)*, edited by: Turekian, K. K., Elsevier,  
528 Oxford, 331-361, 2014.

529 Laaksonen, A., Malila, J., Nenes, A., Hung, H. M., and Chen, J. P.: Surface fractal dimension, water adsorption  
530 efficiency, and cloud nucleation activity of insoluble aerosol, *Scientific Reports*, 6, 25504, doi:  
531 25510.21038/srep25504, 2016.

532 Lambert, A. R., O'Shaughnessy, P. T., Tawhai, M. H., Hoffman, E. A., and Lin, C. L.: Regional Deposition of  
533 Particles in an Image-Based Airway Model: Large-Eddy Simulation and Left-Right Lung Ventilation Asymmetry,  
534 *Aerosol Sci. Technol.*, 45, 11-25, 2011.

535 Lee, B. U., Kim, S. H., and Kim, S. S.: Hygroscopic growth of E-coli and B-subtilis bioaerosols, *J. Aerosol. Sci.*, 33,  
536 1721-1723, 2002.

537 Lin, H., Lizarraga, L., Bottomley, L. A., and Carson Meredith, J.: Effect of water absorption on pollen adhesion, *J.*  
538 *Colloid Interface Sci.*, 442, 133-139, 2015.

539 Longest, P. W., and Holbrook, L. T.: In silico models of aerosol delivery to the respiratory tract - Development and  
540 applications, *Advanced Drug Delivery Reviews*, 64, 296-311, 2012.

541 Möhler, O., DeMott, P. J., Vali, G., and Levin, Z.: Microbiology and atmospheric processes: the role of biological  
542 particles in cloud physics, *Biogeosciences*, 4, 1059-1071, 2007.

543 Ma, Q. X., He, H., and Liu, Y. C.: In Situ DRIFTS Study of Hygroscopic Behavior of Mineral Aerosol, *J. Environ.*  
544 *Sci.*, 22, 555-560, 2010.

545 Melke, A.: The Physiology of Chilling Temperature Requirements for Dormancy Release and Bud-break in  
546 Temperate Fruit Trees Grown at Mild Winter Tropical Climate, *Journal of Plant Studies*, 4, 110-156, 2015.

547 Morris, C. E., Sands, D. C., Bardin, M., Jaenicke, R., Vogel, B., Leyronas, C., Ariya, P. A., and Psenner, R.:  
548 Microbiology and atmospheric processes: research challenges concerning the impact of airborne micro-organisms  
549 on the atmosphere and climate, *Biogeosciences*, 8, 17-25, 2011.

550 Morris, C. E., Conen, F., Alex Huffman, J., Phillips, V., Pöschl, U., and Sands, D. C.: Bioprecipitation: a feedback  
551 cycle linking Earth history, ecosystem dynamics and land use through biological ice nucleators in the atmosphere,  
552 *Glob. Chang. Biol.*, 20, 341-351, 2014.

553 Murray, B. J., O'Sullivan, D., Atkinson, J. D., and Webb, M. E.: Ice nucleation by particles immersed in supercooled  
554 cloud droplets, *Chem. Soc. Rev.*, 41, 6519-6554, 2012.

555 Najera, J. J., Percival, C. J., and Horn, A. B.: Infrared spectroscopic studies of the heterogeneous reaction of ozone  
556 with dry maleic and fumaric acid aerosol particles, *Physical Chemistry Chemical Physics*, 11, 9093-9103, 2009.

557 Noh, Y. M., Lee, H., Mueller, D., Lee, K., Shin, D., Shin, S., Choi, T. J., Choi, Y. J., and Kim, K. R.: Investigation  
558 of the diurnal pattern of the vertical distribution of pollen in the lower troposphere using LIDAR, *Atmos. Chem.*  
559 *Phys.*, 13, 7619-7629, 2013.

560 Pöschl, U., Martin, S. T., Sinha, B., Chen, Q., Gunthe, S. S., Huffman, J. A., Borrmann, S., Farmer, D. K., Garland,  
561 R. M., Helas, G., Jimenez, J. L., King, S. M., Manzi, A., Mikhailov, E., Pauliquevis, T., Petters, M. D., Prenni, A. J.,  
562 Roldin, P., Rose, D., Schneider, J., Su, H., Zorn, S. R., Artaxo, P., and Andreae, M. O.: Rainforest Aerosols as  
563 Biogenic Nuclei of Clouds and Precipitation in the Amazon, *Science*, 329, 1513-1516, 2010.

564 Pappas, C. S., Tarantilis, P. A., Harizanis, P. C., and Polissiou, M. G.: New method for pollen identification by FT-  
565 IR spectroscopy, *Appl. Spectrosc.*, 57, 23-27, 2003.

566 Park, S. S., and Wexler, A. S.: Size-dependent deposition of particles in the human lung at steady-state breathing, *J.*  
567 *Aerosol. Sci.*, 39, 266-276, 2008.

568 Pasanen, A. L., Pasanen, P., Jantunen, M. J., and Kalliokoski, P.: Significance of air humidity and air velocity for  
569 fungal spore release into the air, *Atmos. Environ.*, 25, 459-462, 1991.

570 Petters, M. D., and Kreidenweis, S. M.: A single parameter representation of hygroscopic growth and cloud  
571 condensation nucleus activity, *Atmos. Chem. Phys.*, 7, 1961-1971, 2007.

572 Pope, F. D.: Pollen grains are efficient cloud condensation nuclei, *Environ. Res. Lett.*, 5, 044015, 2010.

573 Posselt, R., and Lohmann, U.: Influence of Giant CCN on warm rain processes in the ECHAM5 GCM, *Atmos.*  
574 *Chem. Phys.*, 8, 3769-3788, 2008.

575 Pratt, K. A., DeMott, P. J., French, J. R., Wang, Z., Westphal, D. L., Heymsfield, A. J., Twohy, C. H., Prenni, A. J.,  
576 and Prather, K. A.: In situ detection of biological particles in cloud ice-crystals, *Nature Geosci.*, 2, 397-400, 2009.

577 Prenni, A. J., Petters, M. D., Kreidenweis, S. M., Heald, C. L., Martin, S. T., Artaxo, P., Garland, R. M., Wollny, A.  
578 G., and Pöschl, U.: Relative roles of biogenic emissions and Saharan dust as ice nuclei in the Amazon basin, *Nat.*  
579 *Geosci.*, 2, 401-404, 2009.

580 Prisle, N. L., Lin, J. J., Purdue, S. K., Lin, H., Meredith, J. C., and Nenes, A.: CCN activity of six pollenkits and the  
581 influence of their surface activity, *Atmos. Chem. Phys. Discuss.*, 2018, 1-26, 10.5194/acp-2018-394, 2018.

582 Pummer, B. G., Bauer, H., Bernardi, J., Bleicher, S., and Grothe, H.: Suspendable macromolecules are responsible  
583 for ice nucleation activity of birch and conifer pollen, *Atmos. Chem. Phys.*, 12, 2541-2550, 2012.

584 Pummer, B. G., Bauer, H., Bernardi, J., Chazallon, B., Facq, S., Lendl, B., Whitmore, K., and Grothe, H.: Chemistry  
585 and morphology of dried-up pollen suspension residues, *Journal of Raman Spectroscopy*, 44, 1654-1658, 2013.

586 Reinmuth-Selzle, K., Kampf, C. J., Lucas, K., Lang-Yona, N., Frohlich-Nowoisky, J., Shiraiwa, M., Lakey, P. S. J.,  
587 Lai, S. C., Liu, F. B., Kunert, A. T., Ziegler, K., Shen, F. X., Sgarbanti, R., Weber, B., Bellinghausen, I., Saloga, J.,  
588 Weller, M. G., Duschl, A., Schuppan, D., and Pöschl, U.: Air Pollution and Climate Change Effects on Allergies in  
589 the Anthropocene: Abundance, Interaction, and Modification of Allergens and Adjuvants, *Environ. Sci. Technol.*,  
590 51, 4119-4141, 2017.

591 Reponen, T., Willeke, K., Ulevicius, V., Reponen, A., and Grinshpun, S. A.: Effect of relative humidity on the  
592 aerodynamic diameter and respiratory deposition of fungal spores, *Atmos. Environ.*, 30, 3967-3974, 1996.

593 Schuttelfield, J., Al-Hosney, H., Zachariah, A., and Grassian, V. H.: Attenuated Total Reflection Fourier Transform  
594 Infrared Spectroscopy to Investigate Water Uptake and Phase Transitions in Atmospherically Relevant Particles,  
595 *Appl. Spectrosc.*, 61, 283-292, 2007a.

596 Schuttelfield, J. D., Cox, D., and Grassian, V. H.: An investigation of water uptake on clays minerals using ATR-  
597 FTIR spectroscopy coupled with quartz crystal microbalance measurements, *J. Geophys. Res.-Atmos.*, 112, D21303,  
598 doi: 21310.21029/22007JD008973, 2007b.

599 Shiraiwa, M., Ueda, K., Pozzer, A., Lammel, G., Kampf, C. J., Fushimi, A., Enami, S., Arangio, A. M., Frohlich-  
600 Nowoisky, J., Fujitani, Y., Furuyama, A., Lakey, P. S. J., Lelieveld, J., Lucas, K., Morino, Y., Pöschl, U.,

601 Takaharna, S., Takami, A., Tong, H. J., Weber, B., Yoshino, A., and Sato, K.: Aerosol Health Effects from  
602 Molecular to Global Scales, *Environ. Sci. Technol.*, 51, 13545-13567, 2017.

603 Skopp, J.: Derivation of the Freundlich Adsorption Isotherm from Kinetics, *J. Chem. Educ.*, 86, 1341, 2009.

604 Sofiev, M., Siljamo, P., Ranta, H., and Rantio-Lehtimäki, A.: Towards numerical forecasting of long-range air  
605 transport of birch pollen: theoretical considerations and a feasibility study, *Int. J. Biometeorol.*, 50, 392, 2006.

606 Song, X. W., and Boily, J. F.: Water Vapor Adsorption on Goethite, *Environ. Sci. Technol.*, 47, 7171-7177, 2013.

607 Steiner, A. L., Brooks, S. D., Deng, C. H., Thornton, D. C. O., Pendleton, M. W., and Bryant, V.: Pollen as  
608 atmospheric cloud condensation nuclei, *Geophys. Res. Lett.*, 42, 3596-3602, 2015.

609 Stuart, B.: *Infrared Spectroscopy: Fundamentals and Applications*, John Wiley & Sons, Ltd., New York, 2004.

610 Sun, J. M., and Ariya, P. A.: Atmospheric organic and bio-aerosols as cloud condensation nuclei (CCN): A review,  
611 *Atmos. Environ.*, 40, 795-820, 2006.

612 Tang, M. J., Cziczo, D. J., and Grassian, V. H.: Interactions of Water with Mineral Dust Aerosol: Water Adsorption,  
613 Hygroscopicity, Cloud Condensation and Ice Nucleation, *Chem. Rev.*, 116, 4205–4259, 2016.

614 Tang, M. J., Chen, J., and Wu, Z. J.: Ice nucleating particles in the troposphere: Progresses, challenges and  
615 opportunities, *Atmos. Environ.*, 192, 206-208, 2018.

616 Taramarcas, P., Lambelet, C., Clot, B., Keimer, C., and Hauser, C.: Ragweed (*Ambrosia*) progression and its health  
617 risks: will Switzerland resist this invasion?, *Swiss Med. Wkly.*, 135, 538-548, 2005.

618 Tong, H. J., Fitzgerald, C., Gallimore, P. J., Kalberer, M., Kuimova, M. K., Seville, P. C., Ward, A. D., and Pope, F.  
619 D.: Rapid interrogation of the physical and chemical characteristics of salbutamol sulphate aerosol from a  
620 pressurised metered-dose inhaler (pMDI), *Chem. Commun.*, 50, 15499-15502, 2014.

621 Womack, A. M., Bohannan, B. J. M., and Green, J. L.: Biodiversity and biogeography of the atmosphere, *Philos.*  
622 *Trans. R. Soc. Lond. Ser. B-Biol. Sci.*, 365, 3645-3653, 2010.

623 Yeh, H. C., Cuddihy, R. G., Phalen, R. F., and Chang, I. Y.: Comparisons of calculated respiratory tract deposition  
624 of particles based on the proposed NCRP model and the new ICRP66 model, *Aerosol Sci. Technol.*, 25, 134-140,  
625 1996.

626 Yeşilbaş, M., and Boily, J.-F.: Particle Size Controls on Water Adsorption and Condensation Regimes at Mineral  
627 Surfaces, *Sci. Rep.*, 6, 32136, doi: 32110.31038/srep32136, 2016.

628 Yin, Y., Levin, Z., Reisin, T. G., and Tzivion, S.: The effects of giant cloud condensation nuclei on the development  
629 of precipitation in convective clouds — a numerical study, *Atmos. Res.*, 53, 91-116, 2000.

630